Agricultural and Forest Meteorology 252 (2018) 88–98

Contents lists available at ScienceDirect

Agricultural and Forest Meteorology

journal homepage: www.elsevier.com/locate/agrformet

Partitioning of ecosystem respiration in a beech forest

Andreas Brændholt[a,*], Andreas Ibrom[a], Klaus Steenberg Larsen[a,b], Kim Pilegaard[a]

[a] DTU Environment, Technical University of Denmark, Denmark
[b] Department of Geosciences and Natural Resource Management, University of Copenhagen, Denmark

ARTICLE INFO

Keywords:
Ecosystem respiration
Flux partitioning
Eddy covariance
Chamber
Seasonality

ABSTRACT

Terrestrial ecosystem respiration (R_{eco}) represents a major component of the global carbon cycle. It consists of many sub-components, such as aboveground plant respiration and belowground root and microbial respiration, each of which may respond differently to abiotic factors, and thus to global climate change. To correctly predict future carbon cycles in forest ecosystems, R_{eco} must therefore be partitioned and understood for each of its various components.

In this study we used the eddy covariance technique together with manual and automated closed-chambers to quantify the individual components of R_{eco} in a temperate beech forest at diel, seasonal and annual time scales. R_{eco} was measured by eddy covariance while respiration rates from soil, tree stems and isolated coarse tree roots were measured bi-hourly by an automated closed-chamber system. Soil respiration (R_{soil}) was measured in intact plots, and heterotrophic R_{soil} was measured in trenched plots. Tree stem (R_{stem}) and coarse root (R_{root}) respiration were measured by custom made closed-chambers.

We found that the contribution of R_{stem} to total R_{eco} varied across the year, by only accounting for 6% of R_{eco} during winter and 16% during the summer growing season. In contrast R_{soil} was approximately half of R_{eco} during winter (52%), spring (45%) and summer (49%), while the contribution increased to 79% during autumn.

Based on observed fluxes in the trenched and intact soil plots, we found that autotrophic R_{soil} accounted for 34% of R_{soil} during summer, i.e. a relatively low fractional estimate compared to findings from other studies. It is likely that dead roots were still decomposing in the trenched soil plots thus causing overestimation of heterotrophic R_{soil}.

Diel R_{stem} and R_{root} measurements showed a distinct pattern during summer with the highest respiration rates around 13:00-15:00 CET for R_{stem}, and the highest respiration seen from 9:00–15:00 for R_{root}. In contrast, R_{soil} showed the lowest respiration during daytime with no clear difference in the diel pattern between the intact and trenched soil plots.

Finally, we calculated annual R_{soil} for different transects, and found that annual R_{soil} estimated from the previously used transect at the site was underestimated due to R_{soil} of the transect not being representative for the spatial heterogeneity of R_{soil} at the site. This highlights the importance of performing a sufficient number of chamber measurements at a site to adequately capture the spatial variation and estimate R_{soil} correctly.

1. Introduction

Ecosystem respiration (R_{eco}) is, after gross primary productivity (GPP), the second largest flux of CO_2 between the biosphere and the atmosphere (Beer et al., 2010; IPCC, 2013). R_{eco} is the sum of respiration from several component of the ecosystem that may respond differently to abiotic factors, and thus to global change (Schimel et al., 2001; Valentini et al., 2003). To correctly understand and predict future ecosystem carbon cycles, R_{eco} must therefore be partitioned into its main sub-components. For forests, major components are aboveground autotrophic respiration from the leaves, branches and stems of the trees, and belowground by the autotrophic respiration from tree roots and the heterotrophic respiration from soil microbes, which together form the soil respiration (R_{soil}) (Hanson et al., 2000; Högberg et al., 2005, Rodeghiero and Cescatti, 2006).

Ecosystem-level net atmospheric exchange of CO_2 (NEE) can be measured on a high temporal scale by the eddy covariance method (e.g. Pilegaard et al., 2001; Wofsy et al., 1993). NEE can be partitioned into GPP and R_{eco}, by various extrapolation methods, one of which uses temperature response functions to extrapolate from measured nighttime respiration rates to estimates of daytime respiration (Reichstein et al., 2005). Whereas eddy covariance provides R_{eco} on a high temporal scale,

* Corresponding author at: Bygning 115, Bygningstorvet, 2800 Kongens Lyngby, Denmark.
E-mail address: andbr@env.dtu.dk (A. Brændholt).

https://doi.org/10.1016/j.agrformet.2018.01.012
Received 30 May 2017; Received in revised form 3 January 2018; Accepted 5 January 2018
0168-1923/ © 2018 Elsevier B.V. All rights reserved.

it does not provide information on the individual components that make up R_{eco}. Instead, chamber based methods can be used to measure the CO_2 flux from the individual components by enclosing a specific part of the ecosystem in a chamber. Typically, chambers of the closed type are used, where the CO_2 flux is calculated based on the near-linear increase in chamber CO_2 concentration during the measurement. Chamber-based methods differ from the eddy covariance method by the smaller spatial coverage (Wang et al., 2010). Eddy covariance covers a large footprint area that may be representative for the studied ecosystem (Nagy et al., 2006). R_{soil}, however, often show a high degree of spatial heterogeneity within the footprint area (Knohl et al., 2008; Webster et al., 2008). At eddy covariance sites, R_{soil} is often determined with manually operated soil chambers (e.g. Wu et al., 2013). To ensure that R_{soil} measurements are representative for the eddy covariance footprint, a sufficient number of measurements must be performed throughout the footprint (Davidson et al., 2002; Savage et al., 2008). By performing the manual chamber measurements distributed throughout the footprint at regular intervals throughout the year, both the seasonal change in R_{soil} and the spatial difference in R_{soil} can be captured to give a good estimate of R_{soil} for the footprint (Savage and Davidson, 2003). However, because of labour intensiveness, manual measurement campaigns rarely capture diel or day to day variability in the fluxes. Automated chamber systems can allow for measurements at much higher temporal resolution, but because of budget constraints usually only a limited number of automated chambers are available causing low spatial coverage of automatic systems. Apart from R_{soil}, measurements of other ecosystem components such as respiration from leaves, branches and tree stems and woody debris lying on the soil surface have been made using both manual and automated chambers (Rodríguez-Calcerrada et al., 2014; Tang et al., 2008; Zhu et al., 2012). As for R_{soil}, these components can show a high degree of spatial and temporal variability throughout the footprint, thus requiring a sufficient number of chamber measurements to capture this variability.

The diel pattern of R_{soil} is generally related to soil temperature (Janssens and Pilegard, 2003; Tang et al., 2005). However, differences in substrate input of carbon from photosynthesis to the soil via the roots can vary across the day (Kuzyakov and Gavrichkova, 2010). Diel changes in substrate input from plants may completely or partly decouple R_{soil} from the diel pattern of soil temperature (Tang et al., 2005). To study the influence of substrate input and the autotrophic contribution from roots to R_{soil}, a trenching can be performed. Here the contribution of roots to R_{soil} is removed by cutting off any roots in a plot and preventing them to grow back (Baggs, 2006; Bond-Lamberty et al., 2011). This stops autotrophic R_{soil} and prevents any input of carbon from photosynthesis. However, the roots are left to decay in the plot and the soil water content may increase (Díaz-Pinés et al., 2010). By comparing plots with intact soil to plots with trenched soil, the heterotrophic and autotrophic components of R_{soil} can be investigated.

The aim of the study was to quantify the CO_2 fluxes from various components of a forest ecosystem on an annual, seasonal, daily and diel scale, and to quantify how the contribution to total R_{eco} of heterotrophic and autotrophic R_{soil} and stem respiration (R_{stem}) vary on a seasonal scale. This was achieved by a combination of the eddy covariance method and manual and automated closed-chamber techniques.

2. Materials and methods

2.1. Site description

Measurements were performed at the Danish ICOS RI site called DK-Sor at 40 m a.s.l. (55°29′13″ N, 55°38″45″ E), where eddy covariance measurements of net ecosystem CO_2 fluxes have been performed continuously since 1996. The climate is temperate maritime with an annual average precipitation and an annual average temperature of 564 mm and 8.5 °C, respectively (Pilegaard et al., 2011).

The forest is dominated by European beech (*Fagus sylvatica* L.) planted in 1921 with small stands of Norway spruce (*Picea abies* (L.) Karst) and European larch (*Larix decidua* Mill.) (Wu et al., 2013). The tree stem density is 288 per hectare with an average tree height of 28 m and an average diameter at breast height (DBH) of 42 cm in 2010. The main rooting depth is 1 m (Pilegaard et al. 2011). However, roots are most frequent at a depth of 0–20 cm (Østergård, 2000). The dense canopy has a peak LAI of 5.0 and the average annual canopy cover duration period is 180 days. The understory is poorly developed due to the well-developed canopy, causing a sparsely vegetated forest floor during most of the year, except during spring when wood anemones (*Anemone nemorosa* L.) are present in part of the forest floor. Depending on the base saturation, the soils are classified as either alfisols or mollisols. The soil carbon pool is 20 kg m^{-2} down to 1 m depth, with a C/N ratio of 20 in the upper organic soil layers, decreasing to 10 in the lower mineral layers (Østergård, 2000). The organic layer is 10–40 cm deep (Pilegaard et al., 2001).

2.2. Eddy covariance measurements

Measurements of NEE were performed at a height of 43 m on the flux tower on the site by a closed-path eddy covariance system based on a Gill HS-50 3D research sonic anemometer (Gill Instruments Limited, Lymington, UK) and a fast response infrared gas analyser LI-7000 (LI-COR Environmental, Lincoln, Nebraska, USA). For details on the raw data processing, see Pilegaard et al., (2011). Nighttime fluxes at insufficient turbulent mixing were removed when the friction velocity (u_*) was lower than 0.1 m s^{-1} and the atmospheric stratification was stable. A dead band of 2 h after re-establishment of turbulent conditions was applied to avoid double accounting from measuring CO_2 fluxes from venting the canopy air space. The removal of data below the u_* threshold value, and periods of system failure, resulted in a data coverage of 54.1% for 2016. The data set was gap-filled and NEE was partitioned into GPP and R_{eco} by the online "REddyProc: Eddy covariance data processing tool" (Department of Biogeochemical Integration, MPI Jena (2017)). In short, the gap-filling procedure follows the approach by Reichstein et al. (2005), and the partitioning of NEE follows the look-up table approach by Reichstein et al. (2005) and the regression approach by Lasslop et al. (2010). This resulted in a continuous data set of half-hourly values of NEE, GPP and R_{eco} for the entire year. From the half-hourly values, the mean daily values were calculated as well as monthly and annual sums of NEE, GPP and R_{eco}.

For the each of the annual sums of NEE, GPP and R_{eco} an uncertainty estimate was calculated. Wu et al. (2013) used five years of data to calculate the relative uncertainties of the annual sums of NEE, GPP and R_{eco} for the DK-Sor site by taking the uncertainties caused by u_* filtering, gapfilling and site heterogeneity into account. By using these relative uncertainties, we calculated the uncertainty estimates for the annual sums of NEE, GPP and R_{eco}.

2.3. Manual closed-chamber soil respiration measurements

R_{soil} was measured manually using a portable 8100-102 10 cm survey chamber connected to a LI-8100A Automated Soil CO_2 Flux System (LI-COR Environmental, Lincoln, Nebraska, USA). R_{soil} was measured on permanently installed soil collars, inserted 4 cm into the soil, on three distinct transects in the footprint area of the eddy covariance measurements. The R_{soil} plots contained litter but no living plants. The first transect, called the inside fence transect, consisted of 12 plots that were positioned within 15 m of the flux tower. The second transect, called the south transect, consisted of 27 plots, which were positioned at 9 locations along a straight line starting 30 m from the flux tower and ending 270 m south of the tower. Each of the 9 locations contained 3 R_{soil} plots. The last transect, called the west transect, consisted of 45 plots. The plots were positioned in groups of three at 15 locations along two parallel lines that were separated by 30 m. The lines started 30 m from the flux tower and ended 210 m to the west. The

location for the south and west transects were chosen to be in the main wind directions and source area for the eddy covariance measurement. See Pilegaard et al. (2011) and Wu et al. (2013) for information about the footprint area and wind direction at the site.

The manual measurements were performed at an interval of two to three weeks, where R_{soil} was measured once per plot with a chamber closure time of 150 s. This resulted in 20 campaign measurements evenly distributed in time during 2016 for each of the transects. The measurements of the three transects were typically performed on two adjacent days between 09:00–16:00 CET, with the inside fence and south transect being measured on the first day, and the west transect being measured on the second day.

2.4. Automated closed-chamber measurements

In addition to the manual chamber measurements, automated closed-chamber measurements of respiration from intact soil, trenched soil, coarse roots and tree stems were performed from 4 January 2016 to 31 December 2016 with a LI-8100A Automated Soil CO_2 Flux System connected to a LI-8150 Multiplexer (LI-COR Environmental, Lincoln, Nebraska, USA). All the automated soil, root and stem chambers were positioned within 15 m from the flux tower. The system performed well through the entire measurement period leading to automatic measurement being performed each day.

R_{soil} was measured by six opaque soil chambers on circular soil collars with a diameter of 20 cm that were permanently inserted 4 cm into the soil. The soil collars contained soil and litter but no aboveground plant parts. One of the soil chambers was an 8100-101 Long-Term CO_2 flux chambers, and five were 8100-104 Long-Term CO_2 flux chambers (LI-COR Environmental, Lincoln, Nebraska, USA). For two of the soil chambers, trenching was first performed on 6 April 2016 to remove the contribution of living roots to the total R_{soil} from the plot. The trenching was done by vertically inserting a spade 25 cm into the soil in a circle around the soil chambers. Roots with a diameter too big to be cut with the spade were cut with a saw. To prevent ingrowth of roots, monthly re-trenching was performed throughout the study period. Thus, the six soil chamber plots consisted of two trenched soil plots and four intact soil plots.

R_{stem} and R_{root} were measured with two custom made coarse root chambers and two custom made stem chambers, respectively. Unlike the LI-COR soil chambers, the root and stem chambers did not open between measurements. Instead, the chamber headspace was continuously flushed between measurements with atmospheric air that was let into the chamber by a small tube. The flow of air to all root and stem chambers was provided by a pump, and the flow to each chamber set to 1 L min^{-1} by a flow meter. This resulted in a near ambient atmospheric air CO_2 concentration in the chambers between measurements. At the beginning of a chamber measurement, the flow of air to the specific chamber was stopped by automatically closing a normally open solenoid valve that was placed on the flush tube going to the chamber. Thus, the chambers were closed during measurements.

The two root chambers were made of transparent acrylic glass and were cylindrical in shape with an inner length of 24 cm and an inner diameter of 7 cm giving a volume of 923 cm^3. Before assembly the cylinder was cut in two halves in the longitudinal axis. A 10 cm long tube with an inner diameter of 0.5 cm, and a filter in the end was attached to the chamber, which acted as a vent to the atmosphere. The chambers were installed in June 2015. For each chamber a suitable coarse root from a soil depth of 5–10 cm was carefully exposed, and the root was rinsed by tap water. The diameter of root was measured, and the root volume and root surface area was calculated. The root was placed in the one half of the cylinder and the other half of the cylinder was placed on top. In each end of the cylinder, the root went through a hole. The two half cylinders were sealed to each other and the hole around the root in each end was sealed with Blu-tack. Following this, the chamber was covered with soil.

The two stem chambers were cylindrical and made of polypropylene, with an inner diameter of 15 cm and an inner height of 10 cm, giving a volume of 1757 cm^2. A 10 cm vent tube with an inner diameter of 0.5 cm, and a filter in the end was attached at the bottom of the chamber. The chambers were attached to the smooth stem surfaces of two beech trees at a height of 1.3 m by a rubber extrusion with a u-profile that was attached to the chamber and sealed with silicone. The chamber was held in place on the stem by adjustable straps.

The ten chambers were connected to the LI-8100A/ LI-8150 in a multiplexed setup, and the system was set up in a repeated automated two-hour cycle during which a measurement of each of the soil, root and stem chambers was performed. The chamber closure time was set to 5 min and the pre-purge and post-purge times were set to 40 s for all chambers.

2.5. Chamber flux calculation and up-scaling of fluxes

All data analysis of the chamber based CO_2 fluxes and post-processing of the eddy covariance data was done using R version 3.2.0 (R Core Team, 2014).

CO_2 fluxes for all chamber measurements were calculated for each individual measurement on a time and area basis by fitting the non-linear equation by Hutchinson and Mosier (1981) with the nlsLM function (minpack.lm package) for model fitting in R (Elzhov et al., 2016). For the manual chamber measurements, the first 20 s after chamber closure were discarded from the flux calculation (the dead band), whereas the dead band was set to 100 s for the automated chamber measurements because an external analyser (used in another study) was attached in parallel with the LI-8100/LI-8150 system, causing increased system volume and therefore increased system response time.

The calculated automated chamber fluxes from soil, stem and coarse roots were quality flagged first by removing fluxes with an $r^2 < 0.80$ of the fit. Following this, the automated soil fluxes, but not stem and root fluxes, were further quality flagged by removing measurements performed at low u_*, where soil fluxes measured by the LI-8100A/LI-8150 system at the site have been found to be overestimated (Brændholt et al. 2017). In short, the automated soil chamber fluxes were compared with u_* measured at the flux tower. From a plot of the fluxes against u_*, a threshold value of 0.2 m s^{-1} was determined visually, as where the decrease of fluxes in response to an increase in u_* levelled off. Fluxes below the u_* threshold value were removed from further analysis. In total the quality control removed 16.3% of the automated root and stem chamber measurements and 44.9% of the automated soil chamber measurements, leaving 30,124 automated chamber measurements for further analysis. For the manual chamber measurements no quality control was applied in the post processing. Instead the quality control was done in the field following a measurement. If the coefficient of variance of the flux, provided by the LI-COR software, was higher than 1.4%, the measurement was discarded and an extra measurement was performed on the plot.

From the quality controlled flux chamber measurements different estimates for the annual CO_2 fluxes were calculated for both the manual and automated measurements following the procedure described by Brændholt et al. (2017). For the manual measurements, annual soil CO_2 fluxes were calculated both for the inside fence transect, the south transect and the west transect.

For each transect, the manual fluxes were used to parameterize an empirical model of R_{soil} as a function of soil temperature as described by Lloyd and Taylor (1994):

$$R_s = R_{283} \exp\left[-E_0\left(\frac{1}{T_s + 273.15 - T_0} - \frac{1}{T_s - T_0}\right)\right] \quad (1)$$

where T_0 and E_0 are fitted parameters, T_s is soil temperature measured at 5 cm depth and R_{283} is the base respiration at a soil temperature of

10 °C. The model was fitted with nlsLM in the R package minpack.lm (Elzhov et al., 2016) that uses a nonlinear least squares regression based on a Levenberg–Marquardt algorithm. By using soil temperature at 5 cm depth measured continuously at the site as model driver input, a continuous one-year time series of mean daily R_{soil} was calculated. A potential soil temperature bias could occur if the soil temperature continuously measured inside the fence at the site, which was used for modelling of the annual CO_2 fluxes, systematically differed from the soil temperatures of the manually measured soil respiration plots. However, no systematic soil temperature difference was found, e.g. exemplified by a mean annual soil temperature inside the fence of 8.4 °C compared to mean annual soil temperatures of 8.7 and 8.2 °C for the south transect and west transect, respectively.

For the automated measurements, annual mean CO_2 fluxes were calculated for the four intact soil plots, the two trenched soil plots, the two root plots and the two stem plots, respectively. Each of the annual CO_2 fluxes was calculated by first averaging the bi-hourly fluxes on a monthly basis, providing a diel pattern of fluxes for each month. From this, a daily mean flux was calculated on a monthly basis at the average of the bi-hourly values. Monthly fluxes were calculated as the sum of the daily soil fluxes in the respective month, and the annual flux was calculated as the sum of the 12 months.

The uncertainties of the annual soil CO_2 fluxes based on the manual chamber for each of the three transects were estimated by the approach used in Wu et al. (2013), which is based on Van Oijen et al., (2005). In short, for each transect a Bayesian calibration was used to quantify the uncertainty of the model predictions, for which a Markov Chain Monte Carlo (MCMC) Metropolis-Hastings random walk algorithm was used. We performed 50,000 MCMC iterations from which the prior parameter distributions were sampled. Different annual soil CO_2 fluxes were calculated using the estimated posterior parameter distributions, and the standard deviation of the annual soil CO_2 fluxes was interpreted as the uncertainty of the annual soil CO_2 flux for a given transect.

R_{stem}, calculated on a stem surface area, was scaled up to the soil surface area by using site data on tree density, tree height and DBH. The tree height and DBH were measured for 54 beech trees during March 2017. For each of the measured trees, the surface stem area was calculated as the surface area of a cylinder with the measured height and a diameter of 0.71 times the measured DBH. This diameter was derived from a form factor for European beech that describes the relationship between the stem ground area at breast height and the volume of wood contained in the stem and branches above a diameter of 5 cm (Landesverwaltungsamt Sachsen-Anhalt (2011)). The average stem surface area calculated from the sampled trees was multiplied with the tree density of 288 stems ha^{-1} to get the stem surface area scaled on a soil surface area. From this the measured R_{stem} on a stem surface area could be converted to a CO_2 flux on a soil surface area.

The uncertainties of the annual soil CO_2 fluxes for the intact soil, trenched and stem measured by the automated chamber were estimated by formal error propagation that took the uncertainties of the various steps in the calculation of the annual fluxes into account. For the annual stem flux, an extra level of uncertainty was included in the calculation that accounted for the uncertainty of the up-scaling of the fluxes from stem surface area to soil surface area. For this, we assumed an uncertainty of 30% in the stem surface area calculated from the measurements of tree height and DBH.

3. Results

3.1. Annual CO_2 budgets

Different annual CO_2 budgets were calculated for different components of the forest from both the tower based eddy covariance and the automated and manual closed-chamber measurements.

The gap-filled annual NEE calculated from the eddy covariance measurement at a height at 43 m on the flux tower was

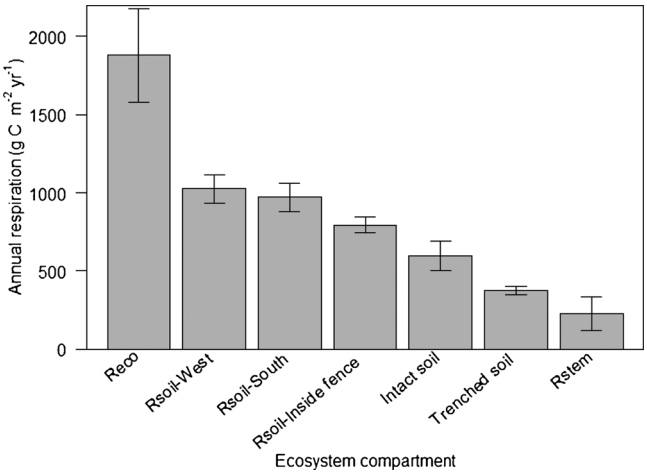

Fig. 1. Annual respiration for the different components of the ecosystem, with the estimated uncertainties shown by error bars. From left to right the bars show: $R_{eco,}$ R_{soil} at the west transect, R_{soil} at the south transect, R_{soil} at the inside fence transect, R_{soil} at the intact soil plots measured by the automated chambers, R_{soil} at the trenched soil plots measured by the automated chambers and R_{stem}. The annual estimated GPP was $2272 \pm 136\ g\,C\,m^{-2}\,yr^{-1}$.

$-391 \pm 63\ g\,C\,m^{-2}\,yr^{-1}$, and the estimated GPP and R_{eco} were 2272 ± 136 and $1882 \pm 301\ g\,C\,m^{-2}\,yr^{-1}$, respectively (Fig. 1).

Different estimates of annual R_{soil} were calculated based on the manual closed-chamber measurements that were used to parameterize the Lloyd and Taylor model (Fig. 1). The lowest annual R_{soil} of $794 \pm 51\ g\,C\,m^{-2}\,yr^{-1}$ was found for the inside fence transect, where the plots were positioned within a distance of 15 m from the eddy flux tower. The annual R_{soil} from the two transects, with soil plots distributed in the forest, were both higher with an annual R_{soil} of $1024 \pm 89\ g\,C\,m^{-2}\,yr^{-1}$ for the west transect and an annual R_{soil} of $972 \pm 90\ g\,C\,m^{-2}\,yr^{-1}$ for the south transect.

The average annual R_{soil} based on the automated closed-chamber measurements every two hours was $597 \pm 93\ g\,C\,m^{-2}\,yr^{-1}$ for the four automated chambers with intact soil and, while the average annual R_{soil} for the two automated chambers containing trenched soil was $375 \pm 29\ g\,C\,m^{-2}\,yr^{-1}$, accounting for 63% of R_{soil} for the intact soil plots.

The annual up-scaled stem CO_2 on a soil surface area basis was 264 ± 88 and $191 \pm 64\ g\,C\,m^{-2}\,yr^{-1}$ for the two automated stem chambers, respectively, resulting in an average of $227 \pm 108\ g\,C\,m^{-2}\,yr^{-1}$ (Fig. 1). This was equivalent to $258 \pm 15\ g\,C\,m^{-2}\,yr^{-1}$ on a stem surface area basis.

Compared to the annual estimate of R_{eco} from the eddy covariance measurements, the annual R_{soil} constituted 43, 55 and 52% from the manually measured inside fence transect, the west transect and the south transect, respectively, while the annual R_{soil} based in the intact soil plots and trenched soil plots measured automatically constituted 32 and 20% of R_{eco}, respectively. The average stem CO_2 flux constituted 12% of R_{eco}.

3.2. Seasonal forest respiration

R_{eco}, R_{soil} and R_{stem} generally followed the same pattern throughout the year with the lowest respiration rates during the cold winter months and the highest rates during the warm summer months (Figs. 2 and 3). However, the individual contribution of R_{soil} and R_{stem} to the total R_{eco} differed between the seasons. R_{stem} showed a high seasonality in its contribution to the total R_{eco} contributing only 6% of R_{eco} during the winter months of January, February and December. A similar low contribution of 7% was seen during the spring months of March, April and May. However, during the summer months of June, July and August the contribution of R_{stem} increased to 16%. In the autumn months

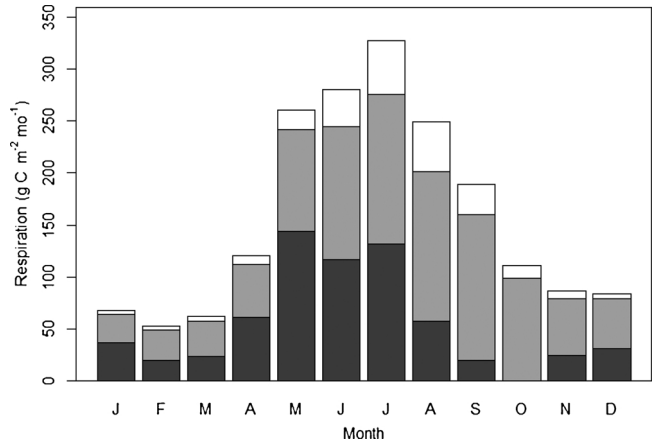

Fig. 2. R_{eco} (total bar height) partitioned into the component respiration rates from R_{soil} (grey) and R_{stem} (white) on a surface area basis for each month of 2016. The black bars represent the remaining R_{eco} after R_{soil} and R_{stem} have been subtracted, i.e. from tree branches and leaves. For the monthly R_{soil}, the average of the manual closed-chamber measurements of the south and west transect is shown. Note, that for October, R_{eco} was 11.9 g C m^{-2} yr^{-1} lower than the sum of R_{stem} and R_{soil}.

of September, October and November the contribution gradually decreased from 16% in September to a level of 9% in November, close to the winter level. The monthly pattern of contribution of R_{soil} to the total R_{eco} differed from R_{stem}. Here winter, spring and summer were fairly similar contributing 52, 45 and 49% to R_{eco}, respectively. However, R_{soil} during the autumn months differed from the rest of the year by contributing 79% to the total R_{eco}.

R_{root}, which was measured for two coarse roots, was not scaled up to the soil surface area because of the various contributions of roots of different sizes to total root respiration.

3.3. Effect of trenching

The annual average R_{soil} for the two trenched soil plots measured by the automated chambers was 63% of annual average R_{soil} for the four intact soil plots. However, the trenching was not performed until 5 April 2016. To investigate the effect of the trenching on R_{soil}, we looked at R_{soil} before and after the trenching. Before the trenching R_{soil} of the trenched plots was 77% of the R_{soil} for the intact soil. However, for the remaining part of the year following the trenching, R_{soil} for the trenched plots decreased to 61% of the intact soil plots.

The course of R_{soil} generally followed the same pattern throughout the year for both the intact and trenched soil plots, by following changes in soil temperature (Fig. 3). However, during the months of June, July and August where GPP was highest (Fig. 4), the intact soil plots reached higher levels of R_{soil} with R_{soil} of the trenched soil plots only being 51% of the intact plots. R_{soil} of one of the intact soil plots differed by showing a rapid increase in R_{soil} during April and May, but then decreasing again to a level similar to the remaining intact soil plots (Fig. 3). For October, November and December during autumn and winter, where GPP was low to near zero μmol m^{-2} s^{-1}, R_{soil} of the intact soil plots decreased to almost the level of the trenched soil plots, with R_{soil} of the trenched plots being 83% of the intact plot, a higher level than the pre-trenching level of 77%.

3.4. Stem respiration and GPP

A rapid increase in GPP was seen in May following the leaf out of the deciduous beech trees (Fig. 4). GPP peaked in June and the high GPP continued into July, following by lower GPP in August and September. A similar rapid increase in May was not seen for the two R_{stem} plots. Instead, a slower increase was seen in May followed by a peak in R_{stem} in July and August. During autumn, however, the decrease in R_{stem} did seem to follow the decrease in GPP. Instead of following GPP, the course of R_{stem} followed the course of R_{soil} during spring, summer and autumn (Fig. 4). However, during summer a higher day to day variability was seen for R_{soil} compared to R_{stem}.

3.5. Diel patterns of CO_2 fluxes

The automated chamber measurements performed every two hours throughout the year allowed for investigating the diel patterns of R_{stem}, R_{root} and R_{soil} for both the trenched and intact soil plots for the different seasons of the year (Fig. 5).

Although R_{soil} was higher for the intact soil plots than for the trenched plots, the diel pattern of R_{soil} generally exhibited the same pattern for both the intact Fig. 5a–d) and the trenched soil plots (Fig. 5a–d). During winter, R_{soil} was generally higher during daytime than during nighttime. For spring and autumn, however, no clear diel pattern was observed. Summer exhibited a diel pattern with generally low R_{soil} during daytime. A peak in R_{soil} was seen early in the morning and late in the evening before midnight. The diel patterns of R_{stem} and R_{root} during summer differed from R_{soil} by having the highest respiration rates during daytime (Fig. 5k, o). R_{stem} peaked at 13:00–15:00 CET, while a longer peak period from 9:00–15:00 was seen for R_{root}. For winter and autumn, no diel pattern was seen for R_{root} (Fig. 5i, l). However, during spring, a similar diel pattern as during summer with

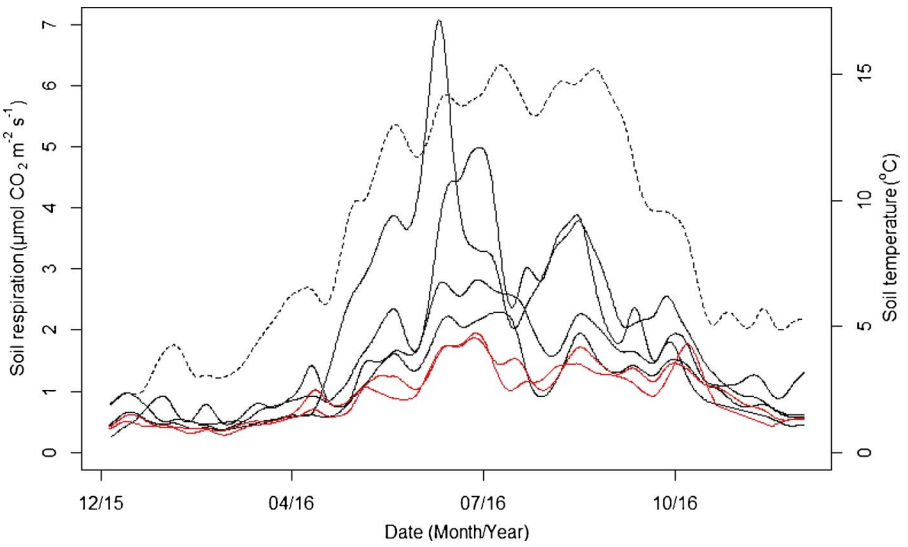

Fig. 3. R_{soil} (solid lines) throughout the year measured by the automated closed-chambers and soil temperature at 5 cm depth (dashed line). The black solid lines show the R_{soil} for the four plots with intact soil and the red solid lines show R_{soil} for the two plots with trenched soil. The lines have been smoothed to show a running five day average. (For interpretation of the references to colour in this figure legend, the reader is referred to the web version of this article.).

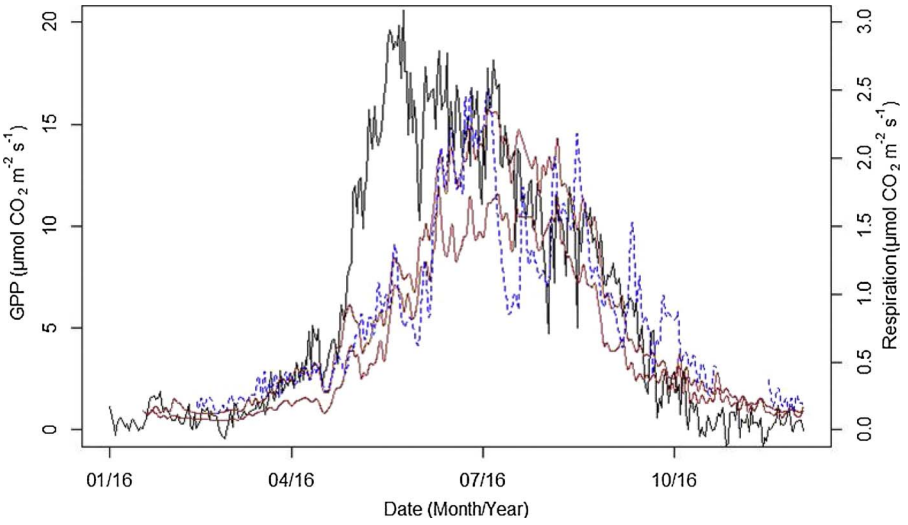

Fig. 4. Mean daily GPP (black line, left y-axis) and R_{stem} (the red lines, right y-axis) throughout the year. For R_{stem} both plots are shown. The blue dashed line shows the mean daily R_{soil} for the intact soil plots measured by the automated closed-chambers. R_{soil} have been multiplied with 0.45 to fit the right respiration scale. (For interpretation of the references to colour in this figure legend, the reader is referred to the web version of this article.).

highest R_{root} during daytime was observed. The diel pattern of R_{stem} during spring and autumn was similar to the diel pattern during summer, although less pronounced, with highest R_{stem} during daytime. R_{stem} for winter, however, showed no diel pattern, which was in contrast to the high daytime R_{stem} seen during the rest of the year.

Soil temperature at 5 cm depth generally showed no diel pattern during winter, summer and autumn (Fig. 6). During spring, however, a moderate diel pattern was observed with highest soil temperatures late in the afternoon or early in the evening and the lowest soil temperatures in the morning. The difference between the highest and lowest diel temperature was, however, only approximately 1 °C.

4. Discussion

4.1. Annual R_{soil} at different transects

We measured R_{soil} at three different transects, which revealed that the annual R_{soil} measured on the inside fence transect was 20% lower than the average annual R_{soil} measured on the west and south transects. Manual R_{soil} measurements on the inside fence transect have previously been used on the site to estimate annual R_{soil}. Wu et al., 2013 found an average annual R_{soil} of 752 ± 30 g C m^{-2} yr^{-1} for a 5 year period, which is close to the 794 ± 51 found in this study. They calculated the aboveground autotrophic respiration to 872 g C m^{-2} yr^{-1}, which they found to be unexpectedly high. They argued that it could be explained if R_{soil} had been underestimated, due to the plots having lower R_{soil} than the average R_{soil} of the footprint. The inside fence transect consisted of 12 plots all positioned within 15 m of the flux tower, at a relatively dry and high ground. In contrast, the two newly established west and south transects, not used in Wu et al. (2013), consisted of 27 and 45 plots, respectively, that were spread out evenly in the forest. R_{soil} and soil moisture measured at both transects showed a higher variation than R_{soil} and soil moisture measured at the inside fence transect (Data not shown). Thus, we argue that the two new transects better represent the spatial variation of R_{soil} in the eddy covariance footprint than the inside fence transect. The annual R_{soil} for the two transects were, however, also similar (972 ± 90 and 1024 ± 89 g C m^{-2} yr^{-1}), constituting 53% of R_{eco}. Knohl et al. (2008) recommended using at least 8 measurement locations spaced randomly throughout the area of interest to get a representative estimate of R_{soil} with sufficient confidence. The two new transects contained 9 and 15 locations throughout the eddy covariance footprint, respectively, each location containing 3 soil collars. Thus, measuring R_{soil} on only one of these transects might be sufficient to cover the spatial variability and get a solid estimation of R_{soil}. The minor difference between the annual R_{soil} from the two transects also supports this. In contrast, the 12 soil collars in the inside fence transect only cover 1 location because they are placed closely together, and therefore do not live up to the recommendations by Knohl et al. (2008).

If the new transects had been used in Wu et al. (2013), the higher R_{soil} would have changed the extremely high estimate of aboveground autotrophic respiration. If we correct R_{soil} in Wu et al. based on the relationship between R_{soil} of the inside fence transect and the other two transects in this study, then the annual R_{soil} increases from 752 to 945 C m^{-2} yr^{-1}. This is turn would lower the estimate of aboveground autotrophic respiration from 872 to 679 g C m^{-2} yr^{-1}, and make the estimates of above and belowground autotrophic respiration more similar as would be expected (Wu et al., 2013).

The annual R_{soil} based on the automated closed-chamber measurements on the 4 intact soil plots was 597 ± 93 g C m^{-2} yr^{-1}, lower than annual R_{soil} of the 3 transects measured by manual chambers. The automated measurements were performed within 15 m from the flux tower, close to the 12 plots of the inside fence transect. Thus, a somewhat similar annual R_{soil} could be expected. However, the annual R_{soil} of the inside transect was 794 ± 51 g C m^{-2} yr^{-1}, higher than the annual R_{soil} based on the automated measurements. The cause for the difference in R_{soil} is unknown. Even though the plots are positioned close to each other, it is possible that spatial heterogeneity within a few metres have caused the difference in R_{soil}. Another possibility is the different closed-chamber systems used, that potentially could lead to different absolute flux values. Lastly, it is possible that the difference between the day time only measurements for the manual chambers and the measurements every two hours for the automated chambers have caused the difference in R_{soil}.

4.2. Comparison of annual respiration

GPP was found to be 2272 ± 136 g C m^{-2} yr^{-1} (Fig. 1). This is high compared to the average of 1881 ± 127 g C m^{-2} yr^{-1} that has previously been found for the site (Wu et al., 2013). We expect an optimal growing season during the study period to be part of the reason for this. No summer drought was observed, which has been found to lower forest growth during summer, thus lowering annual GPP (Ciais et al., 2005). The trees could therefore continue to photosynthesize without any edaphic or climatic reduction during summer. Furthermore, September was exceptionally warm, which allowed the trees to continue photosynthesizing for an additional period at high rates (Fig. 4). R_{eco} was found to be high as well at 1882 ± 301 g C m^{-2} yr^{-1}, which is to be expected due to the commonly found link between GPP and R_{eco} (Mahecha et al., 2010; Peichl et al., 2013) and higher than the 1624 ± 201 g C m^{-2} yr^{-1} found by Wu et al. (2013). Luyssaert et al.

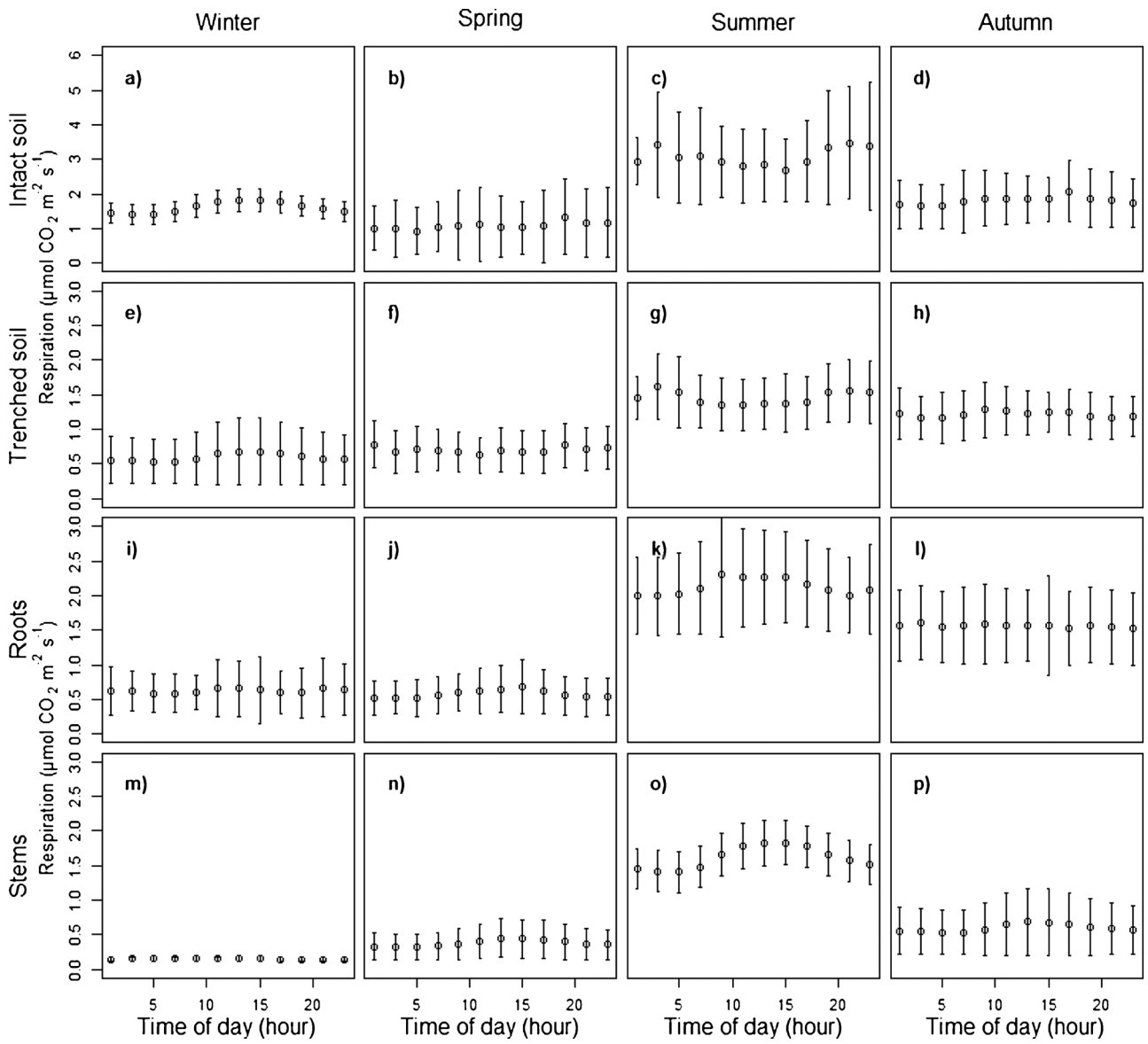

Fig. 5. Seasonally averaged diel patterns of R_{soil} for the intact and trenched soil, R_{root} and R_{stem} measured by the automated closed-chambers for each of the four seasons. Error bars show standard deviation. The seasons of winter, spring, summer and autumn are shown in the four columns from left to right, respectively. The four rows from top to bottom show R_{soil} from intact soil, R_{soil} from trenched soil, R_{root} and R_{stem}, respectively. R_{soil} is shown on a soil surface area basis, while R_{root} and R_{stem} are shown on root surface area and stem surface area basis, respectively.

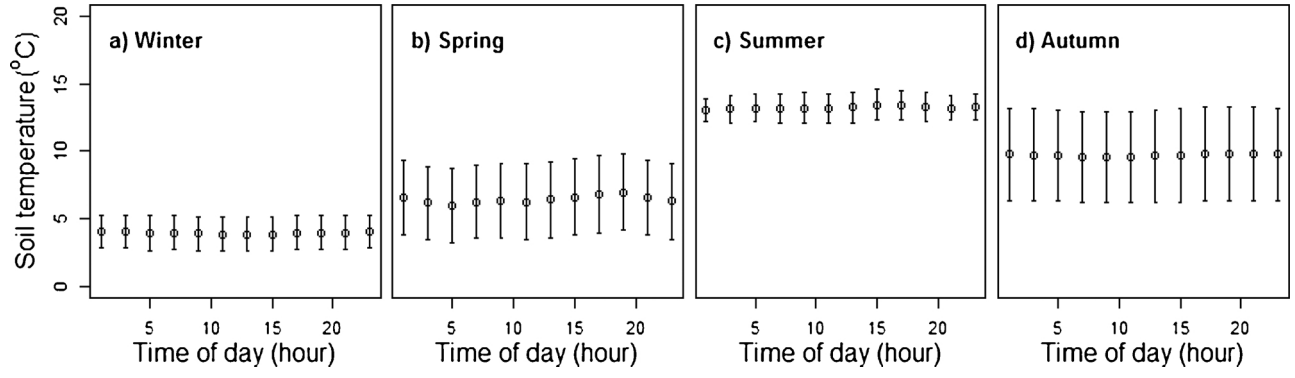

Fig. 6. Seasonally averaged diel pattern of soil temperature (± standard deviation) at 5 cm depth measured by soil thermometers installed close to the automated chambers for winter (a), spring (b), summer (c) and autumn (d).

(2007) assembled a global database of GPP and R_{eco} and reported the average GPP and R_{eco} to be 1375 ± 56 and 1048 ± 64, respectively, for temperate humid deciduous forests, which is much lower than found for the DK-Sor forest. However, we expect GPP and R_{eco} for the DK-Sor forest to be higher because the forest is at its main productive phase with a uniform stand of 100 year-old beech trees with high LAI and a fertile soil. Furthermore, the mild maritime climate and the moderately high latitude close to the northern margin of beech forest's geographic range have relatively long days during the vegetation period. With a canopy process model, Ibrom et al. (2006) showed for two different conifer canopies that the northern, maritime climate in Scotland increased the photosynthetically active radiation use efficiency by 13–14% compared to a more continental climate at a forest site in Central Germany. The reason was longer day lengths, a higher fraction of diffuse radiation and lower vapour pressure deficit at the Scottish site. Compared to the main beech distribution area with many drier and more continental sites, we conclude that the site conditions at the DK-Sor beech forest site allow for comparably high forest productivity.

We found an average annual R_{stem} per unit ground area of 227 ± 108 g C m^{-2} yr^{-1}, which is the first estimate for this flux component at this site (Fig. 1). The quantification of the CO_2 flux from tree stems has not received the same attention as e.g. R_{soil} and R_{eco}, probably associated with the extra work and cost required to construct and operate the custom made stem chambers, and the complications to upscale the measurements to the total stand level. R_{stem} can, however, be a substantial part of R_{eco}, and constituted 12% of R_{eco} in our study. A few studies have addressed the role of R_{stem} for different forest ecosystems (Ceschia et al., 2002; Edwards and Hanson, 1996; Inoue, 2004; Saveyn et al., 2007; Yang et al., 2015; Zha et al., 2004), and a few studies have looked at R_{stem} for beech trees (Ceschia et al., 2002; Damesin et al., 2002; Saveyn et al., 2007). Tang et al. (2008) found that R_{stem} accounted for 13% of R_{eco} in a temperate old-growth hardwood forest in the USA, close to the findings for our forest. Damesin et al. (2002) measured respiration from stem and branches and estimated the annual respiration to be between 325 and 383 g C m^{-2} yr^{-1}, with R_{stem} accounting for approximately 50%. In a review of 18 European forests, Janssens et al. (2000) found that aboveground respiration accounted for 31% of R_{eco}. If half of the aboveground respiration is accounted for by R_{stem} as found by Damesin et al. (2002), then 12% of R_{eco} accounted for by R_{stem} in our study is close to the findings by Janssens et al. (2000).

Upscaling R_{stem} from chamber based measurements to soil surface area for comparison with other ecosystem respiration components can cause considerable up-scaling biases. Three main causes of errors can be identified: Insufficient number of measurements in time to catch the temporal resolution in R_{stem}, insufficient number of measurements to catch the spatial variability in R_{stem} between and within trees, and uncertainty related to scaling up surface measurements to the entire surface of the tree stand. The automatic stem chambers ran continuously throughout the year, thus capturing even the hourly variation of R_{stem}. However, only two stem chambers were available. Annual R_{stem} between the two were slightly different (264 ± 88 and 191 ± 64 g C m^{-2} yr^{-1}) highlighting the possible variation of R_{stem} for different trees. We did the measurement at a stem height of 1.3 m. However, it has for some trees been found that stem CO_2 flux can vary with stem height (Ceschia et al., 2002). This has been found to be caused by various amounts of CO_2 dissolved in the xylem that can diffuse out of the stem and therefore contribute to the apparent CO_2 flux measured by the chamber (Teskey and McGuire, 2002). Some of this CO_2 can be derived from respiration produced elsewhere on the stem, or it can originate from CO_2 produced in the soil that is being dissolved in the soil water, taken up by the roots and transported up through the stem (Aubrey and Teskey, 2009; Bloemen et al., 2013; Teskey and Mcguire, 2007). Differences in R_{stem} along the height of the stems could potentially have influenced the annual estimate of R_{stem}, as well as differences in R_{stem} between different trees. This was, however, not tested in the current study.

4.3. Different seasonal contribution of respiration components

We found a strong seasonal pattern in the contributions of R_{soil} and R_{stem} to R_{eco} (Fig. 2). R_{eco} generally followed the variation in temperature throughout the year with highest R_{eco} during the summer growing season. This is usually seen for other temperate forest with growing season during the warm and relatively wet summer (Janssens et al., 2000), in comparison to e.g. Mediterranean ecosystems where R_{eco} is decoupled from temperature during the hot and dry summers, when water becomes a limiting factor (Matteucci et al., 2015).

The variation in the different seasonal contributions of the individual components to R_{eco} have been explained by differences in phenology, and their individual response to temperature (Migliavacca et al., 2015). R_{stem} experienced dramatic differences in the contribution to R_{eco}, with 6% during winter and 16% during summer. Although following an overall pattern similar to R_{soil} (Fig. 4), R_{stem} was much lower during winter. The deciduous beech trees shed their leaves during autumn and enter a dormant period until spring. During this period they do not photosynthesize, and transpiration is limited to a minimum (Essiamah and Eschrich, 1986). Thus the transport through the xylem and phloem is limited to a minimum and respiration is limited to only the necessary maintenance respiration (Damesin, 2003). However, during the growing season growth respiration may be a significant part of stem respiration, not directly determined by temperature, but by plant phenology (Lavigne and Ryan, 1997). The difference in R_{stem} throughout the year may therefore be larger than what can be expected from a general temperature dependence. Our observation of low R_{stem}, both in absolute terms and in its contribution to R_{eco} during the winter months, fits well with the pattern of tree dormancy during winter, and increased growth respiration during summer. Similar seasonal patterns of R_{stem} have been found in other temperate forests (Acosta et al., 2008; Edwards et al., 2002; Griffis et al., 2004; Shibistova et al., 2002; Yang et al., 2012, 2014). However, most studies do not measure R_{stem} during the winter months, making a full comparison difficult.

R_{soil} from the manual chambers differed dramatically from R_{stem} by showing a fairly similar contribution to R_{eco} during both winter, spring and summer of 52, 45 and 49%, respectively, while the contribution increased to 79% during autumn. Unlike the trees, the microorganisms in the soil do not go into dormancy and can continue to be active and respire, albeit at a slower rate, even during winter (Beverly and Franklin, 2015). Freezing temperatures, which causes the soil to freeze and lower R_{soil} dramatically can occur at our site. However, the winter period during this study was characterized by above-freezing temperatures during daytime for most of the winter; thereby leaving the entire soil column thawed at most times. The very high contribution of R_{soil} during autumn coincided with leaf senescence and litterfall. The input of litter to the soil is significant at the site, and has been found to account for 218 ± 17 g C m^{-2} yr^{-1} (Wu et al., 2013). Although the rate of R_{soil} is determined by temperature, the soil organisms will most often respond by increasing R_{soil} if additional organic matter such as litter is put into the soil (Han et al., 2015). A continuous high R_{soil} or a peak following litterfall has been found for other temperate forest ecosystems (DeForest et al., 2009; Hibbard et al., 2005). Thus, it is likely that the input of litter during autumn has kept R_{soil} at our site high by fuelling heterotrophic respiration. The trees, however, have shed their leaves and begun to enter dormancy, which lowers the relative contribution of plant respiration to R_{eco}.

The automated chamber measurements and the trenching revealed information on the contribution of autotrophic R_{soil} throughout the year. During summer, R_{soil} of the trenched soil plots was only 51% of R_{soil} for the intact plots, while it increased to 83% during autumn, which was comparable to the pre trenching level of 77%. This indicated that autotrophic R_{soil} accounted for 49% during summer. However, before the trenching in April, R_{soil} of the trenched plots was lower than

the intact soil plots, by only accounted for 77%, thus indicating heterogeneous undisturbed R_{soil}. Accounting for this pre trenching difference gives an autotrophic contribution of 34% during summer.

The variation in the seasonal contribution of autotrophic R_{soil} with highest contribution during the plant growing season was expected and has been observed for several ecosystems (Beverly and Franklin, 2015; Pumpanen et al., 2015; Hanson et al., 2000). The major reason for the seasonal pattern of autotrophic R_{soil} is the seasonal pattern of GPP that drives an increase in root respiration during the growing season (Pumpanen et al., 2015). Hanson et al. (2000) reviewed the contribution of autotrophic R_{soil} for different ecosystems and found that the contribution of autotrophic respiration varied from 10% to more than 90%, with a mean value for forests of 45.8%. 50% autotrophic R_{soil} was found in a mixed beech spruce forest in the south of Germany (Andersen et al., 2005). Epron et al. (2001) found a mean autotrophic R_{soil} of 52%, with highest autotrophic rate of 60% in July in a French beech forest. Brumme (1995) found that autotrophic respiration comprised 40% in a central German beech forest. Our trenching was performed in April, making a full comparison for the entire year impossible. Our estimate of an autotrophic contribution of 34% during summer is relatively low compared to prior literature values. However, since the trenching was only performed a few months prior to the measurements, it is possible that decomposing root litter from the severed roots may have contributed to the trenched plots, thereby leading to an overestimated heterotrophic R_{soil} (Díaz-Pinés et al., 2010; Epron et al., 1999; Hanson et al., 2000; Silver et al., 2005; Subke et al., 2006). A second possibility is the presence of deeper living roots below the trenching depth of 25 cm.

Instead of following the variation in GPP, R_{stem} more closely followed R_{soil} and temperature during spring, summer and autumn (Figs. 4 and 3). Thus the high variation in GPP during the growing season was not seen for R_{stem}, which could indicate that the magnitude of R_{stem} was independent from the day to day variations in GPP and the associated high respiration rates that are expected for the photosynthesizing organs. The dependence on temperature is in line with other studies that have found a clear temperature dependence of R_{stem} (Harris et al., 2008; Lavigne et al., 1996; Ryan et al., 1995), although photosynthesis has also been found to partially regulate stem respiration (Zha et al., 2004).

4.4. Diel patterns of respiration

Both R_{stem} and R_{root} showed a clear diel pattern during summer with the highest respiration seen around 13:00–15:00 CET for R_{stem}, and the highest respiration seen from 9:00–15:00 for R_{root} (Fig. 5o, k). The high R_{stem} during the afternoon is consistent with the findings of other studies (Acosta et al., 2008; Teskey and Mcguire, 2007; Zha et al., 2004). This distinct diel pattern have been explained by a temperature response to the diel pattern of temperature (Teskey and Mcguire, 2007). However, other studies have found diel patterns of R_{stem} different from the diel pattern of temperature, which has been suggested to be due to the diel pattern of R_{stem} being modified by photosynthesis and cambium activity independent of temperature (Yang et al., 2014). The diel pattern of R_{stem} during summer in our study followed the diel pattern of air temperature, thus suggesting that temperature is a main determining factor for R_{stem} at our site. This is in line with temperature being the determining factor for R_{stem} at the seasonal scale (Fig. 4, Section 4.3). However, during winter R_{stem} was very low and showed no diel pattern, which could reflect the tree dormancy during this period (Fig. 5m). The high R_{root} during 9:00–15:00 is consistent with the findings of other studies that saw highest R_{root} during daytime, which often has been found to be linked with photosynthesis (Chen et al., 2010; Drake et al., 2008; Lai et al., 2016; Wertin and Teskey, 2008). During daytime, an increase in R_{root} is seen due to respiration of recently fixed photosynthates. During nighttime, however, no photosynthesis takes place, leading to the diel pattern in feeding of photosynthates. Photosynthesis at the DK-Sor site usually peaks at noon, before the peak in temperature (Pilegaard et al., 2001). This is consistent with the peak in R_{root} in this study, thus indicating that photosynthates might in part determine the diel pattern of R_{root} during summer. Interestingly, no diel pattern was seen during winter and autumn (Fig. 5i, l). During winter, no photosynthesis takes place, and only little photosynthesis takes place in autumn, thus only a small amount of photosynthates can alter the diel pattern during these periods. During spring, however, a small peak was seen around 15:00 CET, later than the peak seen during summer (Fig. 5j). Spring was the only season that showed a diel pattern of soil temperature at 5 cm depth (Fig. 6b). Thus, it is possible that the temperature response of R_{root} is dominant during spring.

No clear difference in the diel pattern of R_{soil} was seen between the intact and trenched soil plots (Fig. 5a–h). However, the trenched plots had lower R_{soil} following the trenching, indicating that the autotrophic contribution to R_{soil} had been completely or partly removed from the trenched plots (Section 4.3). Heterotrophic R_{soil} has generally been found to respond to temperature on a seasonal scale, as well as on a diel scale, although a hysteresis on the diel scale between soil temperature and heterotrophic R_{soil} has also been observed (Chen et al., 2009; Song et al., 2015; Zhang et al., 2015). In contrast, autotrophic R_{soil} has often been found to be decoupled from temperature on a diel scale, resulting primarily from substrate transfer to the soil bacteria through carbon exudates from plant roots (Kuzyakov and Gavrichkova, 2010). Similarly to the increase in R_{root} as a result of increased levels of fresh photosynthates, the increase in R_{soil} has been found to lag after photosynthesis (Savage et al., 2013; Tang et al., 2005). Whereas we saw an increase in R_{root} during daytime, we did not see a similar increase in R_{soil} during daytime in the intact soil plot that contained roots. Instead, a lower daytime R_{soil} was seen for both the intact and trenched soil plots. Soil temperature at 5 cm depth generally showed no diel pattern for winter, summer and autumn, which would mean no diel pattern in R_{soil} if only determined by temperature (Fig. 6). It was surprising that no difference was seen between the intact and trenched soil plots. In a previous study at the site, the diel pattern of R_{soil} was investigated for intact soil (Brændholt et al., 2017). A similar diel pattern with lower daytime R_{soil} was observed. However, it was found that the measured soil CO_2 fluxes were influenced by low atmospheric turbulence, which was found to lead to an overestimation of measured soil CO_2 fluxes especially during nighttime, which in turn also biased the diel pattern. In the current study, we removed measurements at low atmospheric turbulence to remove the effect of overestimation of fluxes, as recommended by Brændholt et al. (2017). It is, however, possible that overestimation still plays a role. If this effect is larger than the potential differences in the diel patterns of intact soil and trenched soil, then this effect may overrule the real diel patterns, making it difficult to make a distinction between the diel patterns.

5. Conclusions

In this study we used the eddy covariance technique together with manual and automated closed-chambers to quantify the individual components of ecosystem respiration at diel, seasonal and annual scale. We found that the contribution of R_{stem} to total R_{eco} varied throughout the year, by only accounting for 6% of R_{eco} during winter and 16% during the summer growing season. In contrast, R_{soil} showed a fairly similar contribution to R_{eco} during winter, spring and summer of 52, 45 and 49%, respectively, while the contribution increased to 79% during autumn. We attributed the large difference in the seasonal contribution of R_{stem} to different phenological stages of dormancy and growth experienced for the trees during the year, whereas we attributed the high contribution of R_{soil} in autumn to the large input of litter from the deciduous beech trees.

By the trenching method, we partitioned R_{soil} into its heterotrophic and autotrophic components. We found that autotrophic R_{soil} accounted for 34% of R_{soil} during summer, a relative low value compared to findings from other studies. However, we could not rule out the

possibility that decomposing roots from the trenched soil plots might have led to an overestimated heterotrophic R_{soil}.

Diel R_{stem} and R_{root} showed a clear pattern during summer with the highest respiration seen around 13:00–15:00 CET for R_{stem}, and the highest respiration seen from 9:00–15:00 for R_{root}. In contrast, R_{soil} showed the lowest respiration during daytime R_{soil} with no clear difference in the diel pattern between the intact and trenched soil plots.

Finally, we calculated annual R_{soil} for different transects at the site, and found that annual R_{soil} estimated from the previously used transect at the site was underestimated due to R_{soil} of the transect not being representative for the spatial heterogeneity of R_{soil} at the site. This highlighted the importance of performing a sufficient number of manual chamber measurements at a site to adequately capture the spatial variation in R_{soil}, and thereby to correctly estimate R_{soil}.

Acknowledgement

This study was funded by the Danish Ministry for Research, Innovation and Higher Education, the Danish Council for Independent Research (DFF – 1323-00182).

References

Acosta, M., Pavelka, M., Pokorný, R., Janouš, D., Marek, M.V., 2008. Seasonal variation in CO_2 efflux of stems and branches of Norway spruce trees. Ann. Bot. 101, 469–477.

Andersen, C.P., Nikolov, I., Nikolova, P., Matyssek, R., Häberle, K.H., 2005. Estimating "autotrophic" belowground respiration in spruce and beech forests: decreases following girdling. Eur. J. For. Res. 124, 155–163.

Aubrey, D.P., Teskey, R.O., 2009. Root-derived CO_2 efflux via xylem stream rivals soil CO_2 efflux. New Phytol. 184, 35–40.

Baggs, E.M., 2006. Partitioning the components of soil respiration: a research challenge. Plant Soil 284, 1–5.

Beer, C., Reichstein, M., Tomelleri, E., Ciais, P., Jung, M., Carvalhais, N., Rödenbeck, C., Arain, M.A., Baldocchi, D., Bonan, G.B., Bondeau, A., Cescatti, A., Lasslop, G., Lindroth, A., Lomas, M., Luyssaert, S., Margolis, H., Oleson, K.W., Roupsard, O., Veenendaal, E., Viovy, N., Williams, C., Woodward, F.I., Papale, D., 2010. Terrestrial gross carbon dioxide uptake: global distribution and covariation with climate. Science 329, 834–838.

Beverly, D., Franklin, S., 2015. Heterotrophic and autotrophic soil respiration under simulated dormancy conditions. Open J. For. 5, 274–286.

Bloemen, J., Mcguire, M.A., Aubrey, D.P., Teskey, R.O., Steppe, K., 2013. Transport of root-respired CO_2 via the transpiration stream affects aboveground carbon assimilation and CO_2 efflux in trees. New Phytol. 197, 555–565.

Bond-Lamberty, B., Bronson, D., Bladyka, E., Gower, S.T., 2011. A comparison of trenched plot techniques for partitioning soil respiration. Soil Biol. Biochem. 43, 2108–2114.

Brændholt, A., Larsen, K.S., Ibrom, A., Pilegaard, K., 2017. Overestimation of closed-chamber soil CO_2 effluxes at low atmospheric turbulence. Biogeosciences 14, 1603–1616.

Brumme, R., 1995. Mechanisms of carbon and nutrient release and retention in beech forest gaps. Plant Soil 168–169, 593–600.

Ceschia, É., Damesin, C., Lebaube, S., Pontailler, J.Y., Dufrêne, É., 2002. Spatial and seasonal variations in stem respiration of beech trees (*Fagus sylvatica*). Ann. For. Sci. 59, 801–812.

Chen, D., Zhou, L., Rao, X., Lin, Y., Fu, S., 2010. Effects of root diameter and root nitrogen concentration on in situ root respiration among different seasons and tree species. Ecol. Res. 25, 983–993.

Chen, J.M., Huang, S.E., Ju, W., Gaumont-Guay, D., Black, T.A., 2009. Daily heterotrophic respiration model considering the diurnal temperature variability in the soil. J. Geophys. Res. 114, 1–11 G01022.

Ciais, P., Reichstein, M., Viovy, N., Granier, A., Ogée, J., Allard, V., Aubinet, M., Buchmann, N., Bernhofer, C., Carrara, A., Chevallier, F., De Noblet, N., Friend, A.D., Friedlingstein, P., Grünwald, T., Heinesch, B., Keronen, P., Knohl, A., Krinner, G., Loustau, D., Manca, G., Matteucci, G., Miglietta, F., Ourcival, J.M., Papale, D., Pilegaard, K., Rambal, S., Seufert, G., Soussana, J.F., Sanz, M.J., Schulze, E.D., Vesala, T., Valentini, R., 2005. Europe-wide reduction in primary productivity caused by the heat and drought in 2003. Nature 437, 529–533.

Damesin, C., 2003. Respiration and photosynthesis characteristics of current-year stems of Fagus sylvatica: from the seasonal pattern to an annual balance. New Phytol. 158, 465–475.

Damesin, C., Ceschia, E., Le Goff, N., Ottorini, J.M., Dufrene, E., 2002. Stem and branch respiration of beech: from tree measurements to estimations at the stand level. New Phytol. 153, 159–172.

Davidson, E.A., Savage, K., Verchot, L.V., Navarro, R., 2002. Minimizing artifacts and biases in chamber-based measurements of soil respiration. Agric. For. Meteorol. 113, 21–37.

DeForest, J.L., Chen, J., McNulty, S.G., 2009. Leaf litter is an important mediator of soil respiration in an oak-dominated forest. Int. J. Biometeorol. 53, 127–134.

Department of Biogeochemical Integration, MPI Jena, 2017. REddyProc: Eddy Covariance Data Processing Tool. (Accessed 29 May, 2017). In: http://www.bgc-jena.mpg.de/REddyProc/brew/REddyProc.rhtml.

Díaz-Pinés, E., Schindlbacher, A., Pfever, M., Jandl, R., Zechmeister-Boltenstern, S., Rubio, A., 2010. Root trenching: a useful tool to estimate autotrophic soil respiration? a case study in an austrian mountain forest. Eur. J. For. Res. 129, 101–109.

Drake, J.E., Stoy, P.C., Jackson, R.B., DeLucia, E.H., 2008. Fine-root respiration in a loblolly pine (*Pinus taeda* L.) forest exposed to elevated CO_2 and N fertilization. Plant Cell Environ. 31, 1663–1672.

Edwards, N.T., Hanson, P.J., 1996. Stem respiration in a closed-canopy upland oak forest. Tree Physiol. 16, 433–439.

Edwards, N.T., Tschaplinski, T.J., Norby, R.J., 2002. Stem respiration increases in CO_2-enriched sweetgum trees. New Phytol. 155, 239–248.

Elzhov, V.T., Mullen, K.M., Spiess, A., Bolker, B., 2016. Minpack.lm: R Interface to the Levenberg-Marquardt Nonlinear Least-Squares Algorithm Found in Minpack, Plus Support for Bounds R package version 1.2-0. (Accessed 29 May, 2017). http://CRAN.R-project.org/package=minpack.lm.

Epron, D., Farque, L., Lucot, E., Badot, P.M., 1999. Efflux in a beech forest: the contribution of root respiration. Ann. For. Sci. 56, 289–295.

Epron, D., Le Dantec, V., Dufrene, E., Granier, A., 2001. Seasonal dynamics of soil carbon dioxide efflux and simulated rhizosphere respiration in a beech forest. Tree Physiol. 21, 145–152.

Essiamah, S., Eschrich, W., 1986. Water uptake in deciduous trees during winter and the role of conducting tissues in spring reactivation. IAWA J. 7, 31–38.

Griffis, T.J., Black, T.A., Gaumont-Guay, D., Drewitt, G.B., Nesic, Z., Barr, A.G., Morgenstern, K., Kljun, N., 2004. Seasonal variation and partitioning of ecosystem respiration in a southern Boreal Aspen forest. Agric. For. Meteorol. 125, 207–223.

Hanson, P.J., Edwards, N.T., Garten, C.T., Andrews, J.A., 2000. Separating root and soil microbial contributions to soil respiration: a review of methods and observations. Biogeochemistry 48, 115–146.

Han, T., Huang, W., Liu, J., Zhou, G., Xiao, Y., 2015. Different soil respiration responses to litter manipulation in three subtropical successional forests. Sci. Rep. 5, 18166.

Harris, N.L., Hall, C.A.S., Lugo, A.E., 2008. Estimates of species- and ecosystem-level respiration of woody stems along an elevational gradient in the Luquillo mountains, Puerto Rico. Ecol. Modell. 216, 253–264.

Hibbard, K.A., Law, B.E., Reichstein, M., Sulzman, J., 2005. An analysis of soil respiration across northern hemisphere temperate ecosystems. Biogeochemistry 73, 29–70.

Högberg, P., Nordgren, A., Högberg, M.N., Ottosson-Lofvenius, M., Bhupinderpal, S., Olsson, P., Linder, S., 2005. Fractional contributions by autotrophic and heterotrophic respiration to soil-surface CO_2 efflux in boreal forests. SEB Exp. Biol. Ser. 251–267.

Hutchinson, G.L., Mosier, A.R., 1981. Improved soil cover method for field measurement of nitrous oxide fluxes. Soil Sci. Soc. Am. J. 45, 311–316.

Ibrom, A., Jarvis, P.G., Clement, R.B., Morgenstern, K., Oltchev, A., Medlyn, B., Wang, Y.P., Wingate, L., Moncrieff, J., Gravenhorst, G., 2006. A comparative analysis of simulated and observed photosynthetic CO_2 uptake in two coniferous forest canopies. Tree Physiol. 26, 845–864.

Inoue, A., 2004. Relationships of stem surface area to other stem dimensions for Japanese cedar (*Cryptomeria japonica* D. Don) and Japanese cypress (*Chamaecyparis obtusa* Endl.) trees. J. For. Res. 9, 45–50.

IPCC, 2013. Climate change 2013: the physical science basis. Contribution of Working Group I to the Fifth Assessment Report of the Intergovernmental Panel on Climate Change. Cambridge University Press, Cambridge, United Kingdom and New York, NY, USA, pp. 1535.

Janssens, I., Pilegard, K., 2003. Large seasonal changes in Q_{10} of soil respiration in a beech forest. Glob. Biogeochem. Cycles 9, 911–918.

Janssens, I.A., Lankreijer, H., Matteucci, G., Kowalski, A.S., Buchmann, N., Epron, D., Pilegaard, K., Kutsch, W., Longdoz, B., Grünwald, T., Montagnani, L., Dore, S., Rebmann, C., Moors, E.J., Grelle, A., Rannik, Ü., Morgenstern, K., Oltchev, S., Clement, R., Gudmundsson, J., Minerbi, S., Berbigier, P., Ibrom, A., Moncrieff, J., Aubinet, M., Bernhofer, C., Jensen, N.O., Vesala, T., Granier, A., Schulze, E.D., Lindroth, A., Dolman, A.J., Jarvis, P.G., Ceulemans, R., Valentini, R., 2000. Productivity overshadows temperature in determining soil and ecosystem respiration across European forests. Glob. Change Biol. 7, 269–278.

Knohl, A., Søe, A.R.B., Kutsch, W.L., Göckede, M., Buchmann, N., 2008. Representative estimates of soil and ecosystem respiration in an old beech forest. Plant Soil 302, 189–202.

Kuzyakov, Y., Gavrichkova, O., 2010. Time lag between photosynthesis and carbon dioxide efflux from soil: a review of mechanisms and controls. Glob. Change Biol. 16, 3386–3406.

Lai, Z., Lu, S., Zhang, Y., Wu, B., Qin, S., Feng, W., Liu, J., Fa, K., 2016. Diel patterns of fine root respiration in a dryland shrub, measured in situ over different phenological stages. J. For. Res. 21, 31–42.

Landesverwaltungsamt Sachsen-Anhalt, 2011. Leitfaden zur Vorratsermittlung von Waldbeständen und zur Bewertung forstrechtlicher Sachverhalte. (Accessed 29 May, 2017) (In german). https://lvwa.sachsen-anhalt.de/fileadmin/Bibliothek/Politik_und_Verwaltung/LVWA/LVwA/Dokumente/pressestelle/publikationen/broschueren/vorratsermittlung.pdf.

Lasslop, G., Reichstein, M., Papale, D., Richardson, A., Arneth, A., Barr, A., Stoy, P., Wohlfahrt, G., 2010. Separation of net ecosystem exchange into assimilation and respiration using a light response curve approach: critical issues and global evaluation. Glob. Change Biol. 16, 187–208.

Lavigne, M.B., Franklin, S.E., Hunt Jr, E.R., 1996. Estimating stem maintenance respiration rates of dissimilar balsam fir stands. Tree Physiol. 16, 687–695.

Lavigne, M.B., Ryan, M.G., 1997. Growth and maintenance respiration rates of aspen, black spruce and jack pine stems at northern and southern BOREAS sites. Tree Physiol. 17, 543–551.

Lloyd, J., Taylor, J.A., 1994. On the temperature dependence of soil respiration. Funct. Ecol. 8, 315–323.
Luyssaert, S., Inglima, I., Jung, M., Richardson, A.D., Reichstein, M., Papale, D., Piao, S.L., Schulze, E.D., Wingate, L., Matteucci, G., Aragao, L., Aubinet, M., Beer, C., Bernhofer, C., Black, K.G., Bonal, D., Bonnefond, J.M., Chambers, J., Ciais, P., Cook, B., Davis, K.J., Dolman, A.J., Gielen, B., Goulden, M., Grace, J., Granier, A., Grelle, A., Griffis, T., Grünwald, T., Guidolotti, G., Hanson, P.J., Harding, R., Hollinger, D.Y., Hutyra, L.R., Kolari, P., Kruijt, B., Kutsch, W., Lagergren, F., Laurila, T., Law, B.E., Le Maire, G., Lindroth, A., Loustau, D., Malhi, Y., Mateus, J., Migliavacca, M., Misson, L., Montagnani, L., Moncrieff, J., Moors, E., Munger, J.W., Nikinmaa, E., Ollinger, S.V., Pita, G., Rebmann, C., Roupsard, O., Saigusa, N., Sanz, M.J., Seufert, G., Sierra, C., Smith, M.L., Tang, J., Valentini, R., Vesala, T., Janssens, I.A., 2007. CO_2 balance of boreal, temperate, and tropical forests derived from a global database. Glob. Change Biol. 13, 2509–2537.
Mahecha, M.D., Reichstein, M., Carvalhais, N., Lasslop, G., Lange, H., Seneviratne, S.I., Vargas, R., Ammann, C., Arain, M.A., Cescatti, A., Janssens, I.A., Migliavacca, M., Montagnani, L., Richardson, A.D., 2010. Global convergence in the temperature sensitivity of respiration at ecosystem level. Science 329, 838–840.
Matteucci, M., Gruening, C., Goded Ballarin, I., Seufert, G., Cescatti, A., 2015. Components, drivers and temporal dynamics of ecosystem respiration in a Mediterranean pine forest. Soil Biol. Biochem. 88, 224–235.
Migliavacca, M., Reichstein, M., Richardson, A.D., Mahecha, M.D., Cremonese, E., Delpierre, N., Galvagno, M., Law, B.E., Wohlfahrt, G., Andrew Black, T., Carvalhais, N., Ceccherini, G., Chen, J., Gobron, N., Koffi, E., William Munger, J., Perez-Priego, O., Robustelli, M., Tomelleri, E., Cescatti, A., 2015. Influence of physiological phenology on the seasonal pattern of ecosystem respiration in deciduous forests. Glob. Change Biol. 21, 363–376.
Nagy, M.T., Janssens, I.A., Curiel Yuste, J., Carrara, A., Ceulemans, R., 2006. Footprint-adjusted net ecosystem CO_2 exchange and carbon balance components of a temperate forest. Agric. For. Meteorol. 139, 344–360.
Østergård, J., 2000. Jordbundsdannelse Under bøgeskov og mark ved Lille bøgeskov, Sorø. Master's Thesis. Department of Earth Sciences, University of Aarhus, Denmark (in Danish).
Peichl, M., Sonnentag, O., Wohlfahrt, G., Flanagan, L.B., Baldocchi, D.D., Kiely, G., Galvagno, M., Gianelle, D., Marcolla, B., Pio, C., Migliavacca, M., Jones, M.B., Saunders, M., 2013. Convergence of potential net ecosystem production among contrasting C_3 grasslands. Ecol. Lett. 16, 502–512.
Pilegaard, K., Hummelshøj, P., Jensen, N.O., Chen, Z., 2001. Two years of continuous CO_2 eddy-flux measurements over a Danish beech forest. Agric. For. Meteorol. 107, 29–41.
Pilegaard, K., Ibrom, A., Courtney, M.S., Hummelshøj, P., Jensen, N.O., 2011. Increasing net CO_2 uptake by a Danish beech forest during the period from 1996 to 2009. Agric. For. Meteorol. 151, 934–946.
Pumpanen, J., Kulmala, L., Lindén, A., Kolari, P., Nikinmaa, E., 2015. Seasonal dynamics of autotrophic respiration in boreal forest soil estimated by continuous chamber measurements. Boreal Environ. Res. 20, 637–650.
R Core Team, 2014. R: A Language and Environment for Statistical Computing. R Foundation for Statistical Computing, Vienna, Austria.
Reichstein, M., Falge, E., Baldocchi, D., Papale, D., Aubinet, M., Berbigier, P., Bernhofer, C., Buchmann, N., Gilmanov, T., Granier, A., Grünwald, T., Havránková, K., Ilvesniemi, H., Janous, D., Knohl, A., Laurila, T., Lohila, A., Loustau, D., Matteucci, G., Meyers, T., Miglietta, F., Ourcival, J.M., Pumpanen, J., Rambal, S., Rotenberg, E., Sanz, M., Tenhunen, J., Seufert, G., Vaccari, F., Vesala, T., Yakir, D., Valentini, R., 2005. On the separation of net ecosystem exchange into assimilation and ecosystem respiration: review and improved algorithm. Glob. Change Biol. 11, 1424–1439.
Rodeghiero, M., Cescatti, A., 2006. Indirect partitioning of soil respiration in a series of evergreen forest ecosystems. Plant Soil 284, 7–22.
Rodríguez-Calcerrada, J., Martin-StPaul, N.K., Lempereur, M., Ourcival, J.M., Rey, Mdel Cdel, Joffre, R., Rambal, S., 2014. Stem CO_2 efflux and its contribution to ecosystem CO_2 efflux decrease with drought in a Mediterranean forest stand. Agric. For. Meteorol. 195–196, 61–72.
Ryan, M.G., Gower, S.T., Hubbard, R.M., Waring, R.H., Gholz, H.L., Cropper, W.P., Running, S.W., 1995. Woody tissue maintenance respiration of four conifers in contrasting climates. Oecologia 101, 133–140.
Savage, K., Davidson, E.A., Richardson, D.A., 2008. A conceptual and practical approach to data quality and analysis procedures for high-frequency soil respiration measurements. Funct. Ecol. 22, 1000–1007.
Savage, K., Davidson, E.A., Tang, J., 2013. Diel patterns of autotrophic and heterotrophic respiration among phenological stages. Glob. Change Biol. 19, 1151–1159.
Savage, K.E., Davidson, E.A., 2003. A comparison of manual and automated systems for soil CO_2 flux measurements: trade-offs between spatial and temporal resolution. J. Exp. Bot. 54, 891–899.
Saveyn, A., Steppe, K., Lemeur, R., 2007. Daytime depression in tree stem CO_2 efflux rates: is it caused by low stem turgor pressure? Ann. Bot. 99, 477–485.
Schimel, D.S., House, J.I., Hibbard, K.A., Bousquet, P., Ciais, P., Peylin, P., Braswell, B.H., Apps, M.J., Baker, D., Bondeau, A., Canadell, J., Churkina, G., Cramer, W., Denning, A.S., Field, C.B., Friedlingstein, P., Goodale, C., Heimann, M., Houghton, R.A., Melillo, J.M., Moore, B., Murdiyarso, D., Noble, I., Pacala, S.W., Prentice, I.C., Raupach, M.R., Rayner, P.J., Scholes, R.J., Steffen, W.L., Wirth, C., 2001. Recent patterns and mechanisms of carbon exchange by terrestrial ecosystems. Nature 414, 169–172.
Shibistova, O., Lloyd, J., Zrazhevskaya, G., Arneth, A., Kolle, O., Knohl, A., Astrakhantceva, N., Shijneva, I., Schmerler, J., 2002. Annual ecosystem respiration budget for a *Pinus sylvestris* stand in central Siberia. Tellus 54B, 568–589.
Silver, W.L., Thompson, A.W., McGroddy, M.E., Varner, R.K., Dias, J.D., Silva, H., Crill, P.M., Keller, M., 2005. Fine root dynamics and trace gas fluxes in two lowland tropical forest soils. Glob. Change Biol. 11, 290–306.
Song, W., Chen, S., Zhou, Y., Wu, B., Zhu, Y., Lu, Q., Lin, G., 2015. Contrasting diel hysteresis between soil autotrophic and heterotrophic respiration in a desert ecosystem under different rainfall scenarios. Sci. Rep. 5, 16779.
Subke, J.A., Inglima, I., Cotrufo, M.F., 2006. Trends and methodological impacts in soil CO_2 efflux partitioning: a metaanalytical review. Glob. Change Biol. 12, 921–943.
Tang, J., Baldocchi, D.D., Xu, L., 2005. Tree photosynthesis modulates soil respiration on a diurnal time scale. Glob. Change Biol. 11, 1298–1304.
Tang, J., Bolstad, P.V., Desai, A.R., Martin, J.G., Cook, B.D., Davis, K.J., Carey, E.V., 2008. Ecosystem respiration and its components in an old-growth forest in the great lakes region of the United States. Agric. For. Meteorol. 148, 171–185.
Teskey, R.O., McGuire, M.A., 2002. Carbon dioxide transport in xylem causes errors in estimation of rates of respiration in stems and branches of trees. Plant Cell Environ. 25, 1571–1577.
Teskey, R.O., Mcguire, M.A., 2007. Measurement of stem respiration of sycamore (*Platanus occidentalis* L.) trees involves internal and external fluxes of CO_2 and possible transport of CO_2 from roots. Plant Cell Environ. 30, 570–579.
Valentini, R., Matteucci, G., Dolman, A.J., Schulze, E.D., Jarvis, P.G., 2003. The carbon sink strength of forests in Europe: a synthesis of results. In: In: Valentini, R. (Ed.), Fluxes of Carbon, Water and Energy of European Forests, Ecological Studies 163 Springer, Berlin.
Van Oijen, M., Rougier, J., Smith, R., 2005. Bayesian calibration of process-based forest models: bridging the gap between models and data. Tree Physiol. 25 (7), 915–927.
Wang, M., Guan, D.X., Han, S.J., Wu, J.L., 2010. Comparison of eddy covariance and chamber-based methods for measuring CO_2 flux in a temperate mixed forest. Tree Physiol. 30, 149–163.
Webster, K.L., Creed, I.F., Bourbonnière, R.A., Beall, F.D., 2008. Controls on the heterogeneity of soil respiration in a tolerant hardwood forest. J. Geophys. Res. Biogeosci. 113, 1–15.
Wertin, T.M., Teskey, R.O., 2008. Close coupling of whole-plant respiration to net photosynthesis and carbohydrates. Tree Physiol. 28, 1831–1840.
Wofsy, S.C., Goulden, M.L., Munger, J.W., Fan, S.M., Bakwin, P.S., Daube, B.C., Bassow, S.L., Bazzaz, F.A., 1993. Net exchange of CO_2 in a mid-latitude forest. Science 260, 1314–1317.
Wu, J., Larsen, K.S., van der Linden, L., Beier, C., Pilegaard, K., Ibrom, A., 2013. Synthesis on the carbon budget and cycling in a Danish, temperate deciduous forest. Agric. For. Meteorol. 181, 94–107.
Yang, J., He, Y., Aubrey, D.P., Zhuang, Q., Teskey, R.O., 2015. Global patterns and predictors of stem CO_2 efflux in forest ecosystems. Glob. Chang. Biol. 22, 1433–1444.
Yang, J.Y., Teskey, R.O., Wang, C.K., 2012. Stem CO_2 efflux of ten species in temperate forests in northeastern China. Trees Struct. Funct. 26, 1225–1235.
Yang, Y., Zhao, M., Xu, X., Sun, Z., Yin, G., Piao, S., 2014. Diurnal and seasonal change in stem respiration of Larix principis-rupprechtii trees, northern China. PLoS One 9, 1–7.
Zha, T., Kellomäki, S., Wang, K.Y., Ryyppö, A., Niinistö, S., 2004. Seasonal and annual stem respiration of scots pine trees under boreal conditions. Ann. Bot. 94, 889–896.
Zhang, Q., Katul, G.G., Oren, R., Daly, E., Manzoni, S., Yang, D., Al, Z.E.T., 2015. The hysteresis response of soil CO_2 concentration and soil respiration to soil temperature. J. Geophys. Res. Biogeosci. 120, 1605–1618.
Zhu, L.W., Zhao, P., Ni, G.Y., Cao, Q.P., Zhou, C.M., Zeng, X.P., 2012. Individual-and stand-level stem CO_2 efflux in a subtropical *Schima superba* plantation. Biogeosciences 9, 3729–3737.